Landslides: Evaluation and Stabilization, Lacerda, Ehrlich, Fontoura & Sayao (eds)
© Taylor & Francis Group, London, ISBM 04 1535 665 2

Toward preliminary hazard assessment using DEM topographic analysis and simple mechanical modeling by means of sloping local base level

M. Jaboyedoff
Quanterra, Lausanne, Switzerland

F. Baillifard
Crealp (Research Center on Alpine Environment), Sion, Switzerland

R. Couture
Geological Survey of Canada, Ottawa, On, Canada

J. Locat, & P. Locat
Laval University, Quebec City, Qc, Canada

ABSTRACT: The geomorphological concept of base level is adapted to be useful for landslide hazard assessment. The Sloping Local Base Level (SLBL) is calculated by assuming that all undercut slopes lead to potential unstable volumes. Results for the 1991 Randa rockfall (30 M m^3) area has demonstrated that the SLBL exists. Furthermore, theoretical results for soil slopes are presented showing that SLBL can simulate lystric faults.

1 INTRODUCTION

One of the challenges in landslide hazard assessment is to estimate the volume that can be involved in slope movements before carrying out a detailed field survey. The volumes are usually only defined once the instability is detected. The increasing availability of Digital Elevation Models (DEM) enables researchers to estimate the volumes involved in slope movements, thus limiting expensive field investigations.

Semi-automatic landslide hazard assessment is usually limited to shallow landslides (Pack et al. 1998, Dietrich et al. 2001). Basically, two methods are used: (1) the infinite slope form of the Mohr-Coulomb failure criterion with groundwater table estimates (Pack et al. 1998, Dietrich et al. 2001, 2003) or (2) other instability factors such as landslide inventories or slope maps (Guzzetti et al. 1999). The stability is then estimated for each pixel of the DEM (i.e. each point of the grid) independently from the other ones, with the exception of the groundwater input.

Basically, landslides often involve deep-seated failure surfaces (>10 m) and large volumes (1,000,000 m^3). As shown by some authors, mountain rock slopes are often affected by gravitational movements involving a thick layer of rock (>100 m in thickness), sliding or toppling down to the valley (Nemcŏk 1977, Giraud et al. 1990). This generally occurs when the bottom of the slope is undercut (Terzaghi 1962, Cruden 1976), or affected by dissolutions, (Compagnon et al. 1997). Soil slopes can also be affected by deep-seated sliding surfaces, depending on the angle of the slope and its height (Robitaille et al. 2002).

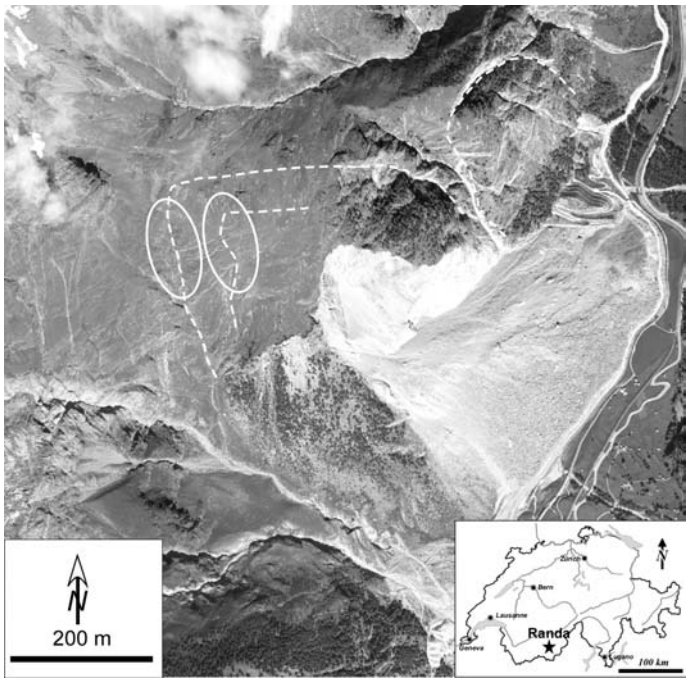

Figure 1. Aerial photograph of the Randa rockfall area. The dashed lines indicate the physical position of the SLBL (SWISSIMAGE© 2004 swisstopo (BA045928)).

The present paper is an attempt to define the position of the potential sliding surfaces, either in rock slopes or in soil slopes from the present topography. The principle of the proposed method is based on the improvement of the geomorphological concept of "base level" (Allaby & Allaby 1990), defined as the lowest level of erosion. The lowest position of a potential sliding surface is defined taking the present topography into account by searching for a surface joining all rivers. This leads to the definition of the maximum volume that can be affected by gravita-

tional movements. Solutions of for soil and rock slopes are discussed. Given a defined volume, slope hazard assessment can be carried out by using a simple mechanical-like model.

2 STUDY AREA

The Randa rockfall is used as a benchmark to illustrate the present approach (Fig. 1). Its general features are now well known and its geomorphological aspects have been studied (Sartori et al. 2003).

Thirty million cubic meters of rocks fell from a rock face near the village of Randa (10 km north of Zermatt, Switzerland) in two main stages: the first one (22 million m^3) on April 18, 1991, and the second one (7 million m^3) on May 9, 1991. The run-out distance was very small compared to the expected one based on volumes (Schindler et al. 1993). The mechanism of the Randa rockfall was mainly controlled by structural features, especially by a large discontinuity lying at the bottom of the cliff. The evolution of the slope surrounding the rockfall presents clear signs of antecedent instabilities (Sartori et al. 2003).

The rockfall scar is situated within the Siviez-Mischabel fold nappe. The base of the scar is made of a Permian intrusion (the Randa orthogneiss) that shapes the main cliffs of the area. The upper part lies within a less competent paragneiss (Escher et al. 1997).

The morphology of the Randa cliff is a spur inherited from glacial age that was affected by old slope movements: (1) a pre-existing landslide and (2) ancient open cracks above the present rockfall scar. These open cracks indicate that the slope is still and was active. In addition, the second rockfall stage was identified as retrogressive erosion. All the changes induced by the first rockfall stage favored both weathering and groundwater circulations that led to second failure.

3 BASICS AND METHODS

3.1 Definition of the sloping local base level

The geomorphological concept of "base level" is defined as the lowest level that can be eroded by a stream (Strahler & Strahler 2002). At regional scale, the base level is defined by the sea level. At local scale, the base level is defined by a lake or by the junction of a tributary and a main river (Allaby & Allaby 1990). The classical base level is not very useful for landslide characterization, because peneplanation involves all erosion processes and a time scale far beyond the scope of landslide hazard assessment.

A typical time scale useful for landslide processes is much shorter, generally less than 50,000 years.

However, assuming that erosion by landsliding can affect only a limited vertical thickness of a slope (i.e. from 0 to approximately 1,000 m) a short-term *local base level* that is sloping can be defined, contrasting with the base level, which is horizontal. As landslides scars are sloping topography, a *sloping local base level* (SLBL) has to be defined with regard to landslides.

This concept means that all slope volumes that are not buttressed at their bottom are liable to slide, at short- or long-term, down towards the valley.

3.2 Classical dynamic slope erosion modeling and geometric approach

Modeling slope erosion is often performed for periods covering million of years (Kooi & Beaumont 1996, Dietrich et al. 2003). It leads to peneplains as a final result. The erosion is often dependent on many parameters, such as relief curvature, slope, altitude uplifts, fluvial or glacial erosion (Young 1972, Thornes & Brunsden 1977). Such modeling leads to a dynamic evolution of the topography with time. It can be applied to present relief and makes it possible to project its evolution for a given period towards the future (Dietrich et al. 2003). These procedures give information on the areas that are more sensitive to erosion, but they do not give any information on the sliding surfaces or the geometry of the landslide.

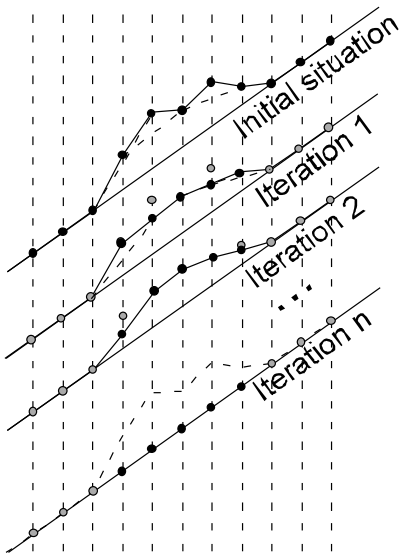

Figure 2. Illustration of some steps of the computation of the SLBL for a 2D-infinite slope containing a spur. The black dots represent the result for a given step and the gray dots represent the previous step(s). Several intermediate steps are missing.

3.3 Geometric approach to find the SLBL

The above approaches are very sensitive to the estimates of each time-dependent parameter such as erosion rates or coefficient of diffusion. The latter is defined as the rate of change of the topography curvature. The basic idea of the approach involving the SLBL is to find, for a given relief at a given time,

the volumes that are liable to be affected by gravitational movements.

Considering a spur along an infinite slope in a 2D-approach, the SLBL corresponds to a line joining the top and the bottom of the spur (Fig. 2). Assuming equidistant z_i altitude data, the SLBL is found by an iterative procedure derived from the background definition of X-Ray diffractions (Sonneveld & Visser 1975). All points located above the mean of their two neighbors are replaced by their mean value. Explicitly, the procedure uses the following conditions:

$$\text{If } z_i > ((z_{i-1} + z_{i+1})/2) \text{ then } z_i = ((z_{i-1} + z_{i+1})/2) \quad (1)$$

The result is a straight line. Introducing a tolerance value C leads to a second-degree curve:

$$\text{If } z_i > (((z_{i-1} + z_{i+1})/2)\text{-C}) \text{ then } z_i = (((z_{i-1} + z_{i+1})/2)\text{-C}) \quad (2)$$

To provide a procedure that produces no holes in the SLBL, two additional conditions can be added:

$$\text{If } z_i > (((z_{i-1} + z_{i+1})/2)\text{-C}) \text{ and } ((((z_{i-1} + z_{i+1})/2)\text{-C}) > z_{i-1} \text{ or } (((z_{i-1} + z_{i+1})/2)\text{-C}) > z_{i+1}) \text{ then } z_i = (((z_{i-1} + z_{i+1})/2)\text{-C}) \quad (3)$$

In 3D, the procedure is similar. The test is simply made by replacing the highest and the lowest value among the four direct neighbors by z_{i-1} and z_{i+1} (Fig. 3).

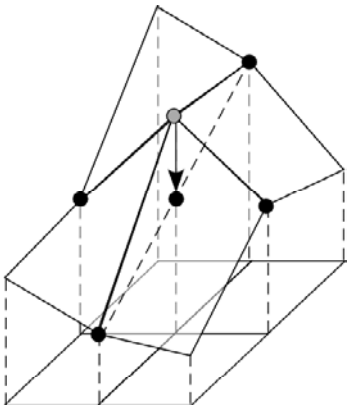

Figure 3. Illustration of the computation of the SLBL in 3D. The arrow indicates the change in altitude of the central point for one iteration.

Some points must be fixed for the computation of the SLBL, otherwise the results is a flat topography. Assuming that the rivers incise directly the rock mass, they are considered as invariant levels in the topography.

The streams are calculated by standard freeware extensions designed for the ArcView program, such as the "basin1" script (ESRI, 2003). A stream is created once a threshold number of pixel contributing to the flow is reached. The base level is thus anchored to the lines defined by the streams. Depending on the position of the upper part of the streams compared to the crest, the highest crests of the mountain range can also be considered as invariant, assuming that summit area experience only small volume rock-falls because of the low force involved. Only large landslides affecting the entire slope can affect crests, but their origin is not the crest.

Volumes and thickness of potential rockslide can be defined by the SLBL. The SLBL changes with the threshold limit assigned to stream initiation. This makes it possible to define different orders of SLBL based on various stream definitions.

The difference in altitude of the SLBL and the topography for each pixel is defined as the residual. The residual is a map depicting the volumes that could be potentially unstable on the SLBL.

From a mathematical point of view, the surface of sliding defined by the SLBL procedure possesses a constant second derivative (curvature).

3.4 Towards a mechanical approach

The volumes located above the SLBL are assumed to slide on the SLBL surface. Within a domain delimited by the streams, every non-invariant pixel applies a force on the pixels below it.

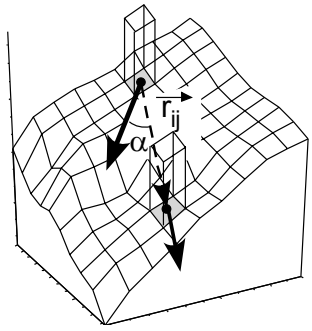

Figure 4. Illustration of how the index of sliding of one pixel that applies a force on another one is computed. The force decreases with the inverse distance between the two pixels.

Assuming that all pixels are sliding, an estimate of the total number of pixels that are pressing on each considered pixel can be computed. The units of shear strength on the SLBL are relative, but make it possible to estimate the index of sliding, i.e. the value that depict for each pixel the state of strength of the cliffs. The index of sliding s_i, for the pixel i is calculated as follows (Fig. 4):

$$s_i \propto \Delta x \times \Delta y \times \rho \times g \left| \left(\vec{v}_i h_i + \sum_{i \neq j} \vec{r}_{ij} \frac{h_j \cos\alpha}{\left|\vec{r}_{ij}\right|^2} \right) \right| \quad (4)$$

Where Δx and Δy are the grid cell size, ρ the density of material, g the constant of terrestrial gravitational acceleration, h_i and hj are the thickness of the layer defined by the SLBL, α the angle between the sliding direction of the pixel j and the vector r_{ij} joining the pixel j and i, and v_i the direction of sliding on the SLBL for the pixel i. The value s_i represents the sum of the contributions of all pixels that potentially apply forces that make sliding i.

4 RESULTS

4.1 2-dimensional theoretical example in soil

In order to demonstrate the applicability of the SLBL to soil slopes, two theoretical examples are shown (Fig. 5).

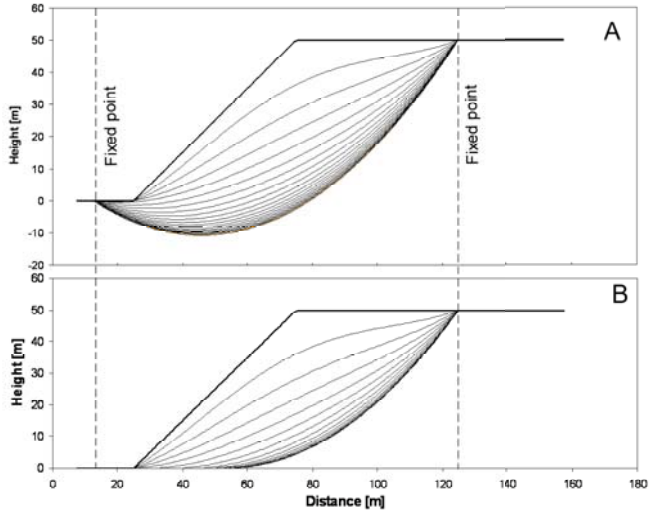

Figure 5. (A) Second order surface generated by the SLBL procedure in soil slope assuming condition 2. (B) Same as (A), but assuming condition 3.

Using the SLBL procedure in 2D, curved sliding surfaces can be created by defining two fixed points, one at the bottom of the slope and one at its top. The example shown in figure 5a uses a 2 m-wide 2D-DEM mesh size, a slope angle of 45°, a slope height of 50 m and a negative tolerance C = -0.0025 m. Points located at 12.5 m and 125 m are chosen invariant. Using condition (2), the final result is a parabolic sliding surface. The different lines indicate different steps of each of the 2000 iterations.

The second example uses condition (3) with C = -0.0025. This leads to a lystric-like fault (Figure 5b).

4.2 The example of the Randa rockfall area

The SLBL was calculated on the area surrounding the Randa rockfall (Fig. 1). The streams were calculated using the "basin1" routine, with 1000 pixels as threshold to initiate a stream. Some of the streams were manually removed, because they were located within the steepest cliffs (Fig. 6).

The results indicate that the Randa rockfall is located within a large volume defined by the SLBL, which can be considered as a potential deep-seated landslide (Fig. 7). Furthermore, the rockfall took place where the residual is the highest (Figs. 7 & 8). The cross-section displaying the SLBL and the topography before and after the Randa rockfalls shows clearly that only part of the volume of the spur was removed during the two Randa rockfall events (Fig. 8). The SLBL in the Randa rockfall area indicates a direction of movement down to the southeast, while the northern part apparently would tend to slide down to the valley eastward (Fig. 6).

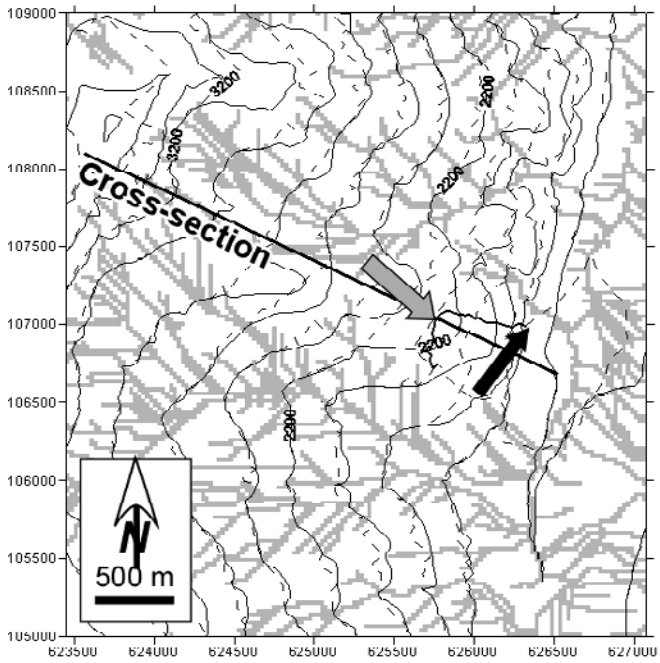

Figure 6. Map displaying the topographic levels (continuous lines) and the SLBL (dashed line). The streams used for the SLBL computation are represented in gray. The Randa rockfall scar is indicated by a black line, and the deposit by a dashed line. The straight line represents the cross-section of Figure 8. The gray arrow indicates the direction of slope movements for the Randa rockfall area indicated by the SLBL and the black arrow is the direction of sliding of the first Randa rockfall event (DHM25© 2004 swisstopo (BA045928)).

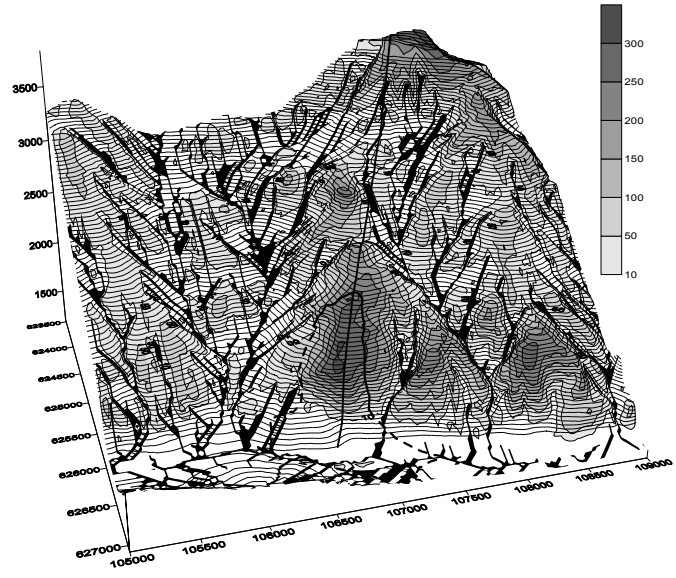

Figure 7. Illustration of the residual, i.e. the difference in altitude between the SLBL and the DEM in meters. The north is on the right. Cross-section and Randa rockfall are indicated. The scar is located where the residual is the highest (DHM25© 2004 swisstopo (BA045928)).

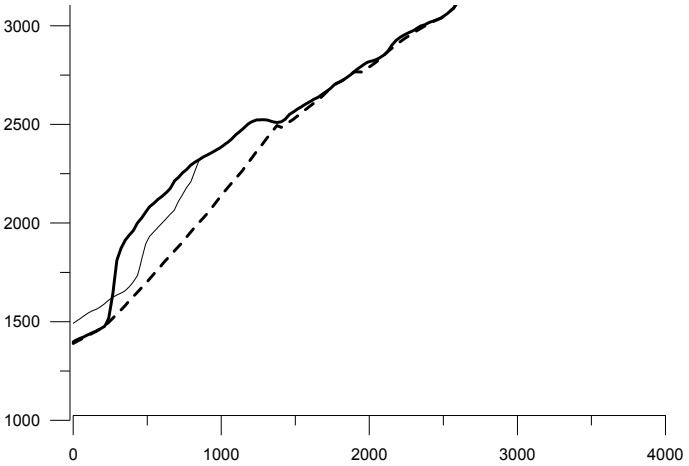

Figure 8. Cross-section of the Randa spur. The bold line is the pre-rockfall topography. The thin line is the present topography including the deposits from both rockfalls. The dashed line is the SLBL obtained from Figure 7.

The trace of the SLBL daylights at the base of the spurs in the channel of streams. This leads to the question: Can the SLBL be observed in the field? Figure 9 shows traces of large sliding surfaces at the top of the spur containing the Randa rockfall. In addition, many open cracks oriented perpendicular to the movement defined by the SLBL can be observed above the present scar (Fig. 9).

Figure 9. Photograph of the upper part of the present Randa spur. The ellipses show the two SLBL of different orders affecting the spur (see Figure 1). The left one corresponds to the SLBL defined on Figure 7.

The spur located at the north of the 1991 rockfall zone presents also an important residual volume defined by the difference between the topography and the base SLBL. A detailed inspection of the aerial photographs (Fig. 1) indicates that a SLBL exists physically because fault traces or rivers emphasize it. Moreover, a rockfall affected the upper part of the cliff using the SLBL as a lateral detachment surface.

Looking at the pseudo-mechanical map, i.e. index of sliding; the rockfall area appears clearly to be the region potentially subjected to the highest shear strength on the SLBL. The value represented on figure 10 is the result of equation (4) divided by $\Delta x \times \Delta y \times \rho \times g$, which is equivalent to the potential shear force existing at the bottom of the considered pixel. The value is given in terms of thickness of residual, the force being equivalent to the weight of this rock column.

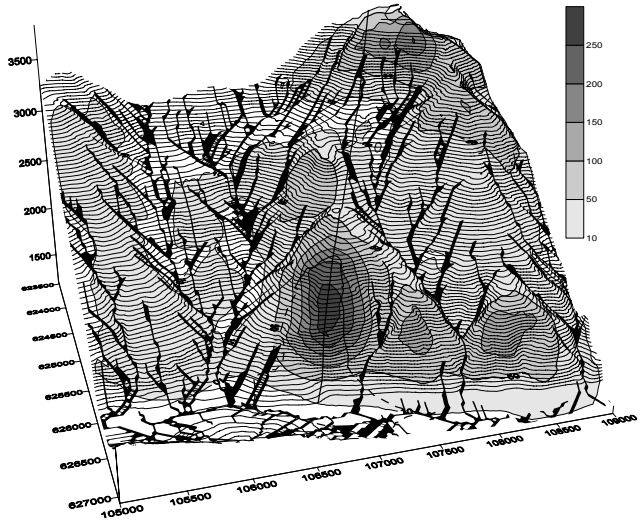

Figure 10. Computation of the sliding index (the black area indicate the higher values) reported to the DEM anterior to the rockfall (DHM25© 2004 swisstopo (BA045928)).

5 DISCUSSION

Considering that all undercut slopes can develop a shear surface equivalent to the SLBL, the concept of SLBL leads to the definition of the volume that could potentially slide down to the valley. In the case of the Randa rockfall, numerical simulations demonstrate that the highest shear strength and the highest relative movements occur at the base of the cliff (Eberhardt et al. 2002). Usually, the bottoms of cliffs are considered as locations that favor fracturing (Castelli 2000).

The slope investigated with the proposed method displays features that demonstrate the physical existence of the SLBL (Fig. 9). It is evident that the concerned volumes are very different depending on the stream order used to define the SLBL.

In our experience, rockfalls occur where residuals are significantly high, taking into account the target volume, implying a relevant number of pixels to initiate the streams. Instabilities presenting a high hazard seem to exist in rock slopes only if they are favored by preexisting structures.

For soil slopes, SLBL can also be defined. But it seems that hazard assessment must be associated with estimations of the mechanical properties of the soil.

The SLBL is a static way to define the present potential instable volumes. In order to go back to dynamical modeling, erosion functions can be used to undercut slopes or to deepen streams in order to cause slope destabilization.

5.1 Implication for rockfall run-out distance

An unexpected result of this study is a hypothesis about the limited run-out distance of the first Randa

rockfall. The overall sliding direction to the southeast defined by the SLBL is different from the direction of sliding defined by the discontinuity dipping down to the northeast (Sartori et al. 2003). Thus, mechanisms involving large-scale slope movements and pre-existing discontinuities that do not have the same directions of movement may have the effect of shortening the run-out distance. This observation supports the hypothesis made by Friedmann et al. (2003), indicating that the directions of rockfall movements and deposits must be the same to obtain large run-out distances.

6 CONCLUDING REMARKS

The roots of the SLBL concept goes back to a concept defined by Terzaghi (1962), which detected deep-seated landslides based on geomorphological arguments. The present approach is a contribution for rock slopes, as well as for soil slopes hazard assessment. Further work must be performed in order to document the existence of the SLBL.

6.1 Future developments

The present approach does not take into account the groundwater table effect on stability; this must be integrated in a more complex mechanical modeling as well as, the routines used to define the SLBL must be improved in order to obtain a more smoothed surface. The drainage network or the routine to define the DEM invariant must also be refined, in order to introduce further geomorphological criteria. Finally, the mechanical modeling must be improved: finite elements or other methods must be applied.

Acknowledgments: The first author thanks the Société Académique Vaudoise for its grant. We thank Jan Aylsworth, from Geological Survey of Canada, for substantially improving our manuscript.

REFERENCES

Allaby, A. & Allaby, M. 1990. *The concise Oxford dictionary of earth sciences*: 410. Oxford Univ. Press.

Castelli, M. 2000. A simplified methodology for stability analysis of rock slopes with non-persitent discontinuity systems. In Yufin (ed.), *Geoecology and computers*: 185- 190. Rotterdam: Balkema.

Compagnon, F., Guglielmi, Y., Follacci, J.-P. & Ivaldi, J.-P. 1997. Approche chimique et isotopique de l'origine des eaux en transite dans un grand mouvement de terrain : exemple du glissement de la Clapière (Alpes-Maritimes, France). C. R. Acad. Sciences, Earth & Planetary sciences, 325: 565-570.

Cruden, D.M. 1976. Major slides in the Rockies. *Can. Geotech. J.* 13: 8-20.

Dietrich, W. E., Bellugi, D., Sklar, L., Stock, J. D., Heimsath, A. M., & Roering, J. J. 2003. Geomorphic transport laws for predicting landscape form and dynamics. In Wilcock, P., & Iverson, R. (eds), *Prediction in Geomorphology*, *Geophysical Monograph* 135: 103-132.

Dietrich, W.E., Bellugi, D., & Real de Asua, R. 2001. Validation of the shallow landslide model, SHALSTAB, for forest management. In Wigmosta, M..S. & Burges, S. J. (eds), *Land Use and Watersheds: Human influence on hydrology and geomorphology in urban and forest areas; Amer. Geoph. Union, Water Science and Application* 195-227.

Eberhardt, E., Stead, D., Coggan, J. & Willenberg, H. 2002. An integrated numerical analysis approach applied to the Randa rockslide. In Rybár, J., Stemberk, J. & Wagner, P. (eds), *Proceedings of the 1st European Conference on Landslides,* Prague: 355-362. Rotterdam: Balkema.

Escher, A., Hunziker, J.C., Marthaler, M., Masson, H., Sartori, M., & Steck, A. 1997. Geologic framework and structural evolution of the Western Swiss-Italian Alps. In Pfiffner, O.A., Lehner, P., Heitzmann, P., Mueller, S. & Steck, A. (eds), *Deep structure of the Swiss Alps (Results of the NRP 20)* 205-221.

ESRI, 2003. http://arcscripts.esri.com.

Friedmann, S. J., Kwon, G. & Losert, W. 2003. Granular memory and its effect on the triggering and distribution of rock avalanche events. *J. Geophys. Res.* 108: 2380, doi:10.1029/2002JB002174.

Guzzetti, F., Carrara, A., Cardinali, M. and Reichenbach, P., 1999. Landslides hazard evaluation: a review of current techniques and their application in a multi-scale study, Central Italy. Geomorphology, 31: 181-216.

Giraud, A., Rochet R., & Antoine, P. 1990. Processes of slope failure in crystallophyllian. *Engineering Geol.* 29: 241-253.

Kooi, H. & C. Beaumont 1996. Large-scale geomorphology; classical concepts reconciled and integrated with contemporary ideas via a surface-processes model, *J. Geoph. Res.*, 101, 3361-3386

Nemcŏk, A. 1977. Geological/tectonic structures: An essential condition for genesis and evolution of slope movement. *Bull. Assoc. Engineering*: 127-130.

Pack, R.T., Tarboton, D.G. & Goodwin, C.N. 1998. The SINMAP Approach to Terrain Stability Mapping, *Paper Submitted to 8th Congress of the International Association of Engineering Geology, Vancouver, British Columbia, Canada 21-25 September 1998*.

Robitaille, D., Demers, D, Potvin, J. & Pellerin, F. 2002. Mapping landslide-prone areas in the Saguenay region, Quebec, Canada. In McInnes, R.G. & Jakeways, J. (eds), *Instability: planning and management.*

Sartori, M., Baillifard, F., Jaboyedoff, M. & Rouiller, J.-D., 2003. Kinematics of the 1991 Randa rockfall (Valais, Switzerland). *Natural Hazards and Earth System Sciences* 3(5): 423-433.

Schindler, C., Cuenod, Y., Eisenlohr, T. and Joris, C.-L. 1993. Die Ereignisse vom 18. April und 9. Mai 1991 bei Randa (VS) - ein atypischer Bergsturz in Raten. Eclogae geol. Helv., 86/3, 643-66.

Sonneveld, E.J., & Visser, J.W. 1975. Automatic collection of Powder data from photographs. *J. Appl. Cryst.* 8: 1-7.

Strahler,A.H. & Strahler, A. 2002. Introducing Physical Geography, 3rd Edition. J. Whiley.

Terzaghi, K. 1962. Stability of slopes on hard unweathered rock. *Geotechnique* 12: 251-263.

Thornes, J.B. & Brunsden, D. 1977. *Geomorphology & Time*: 208. Methuen & Co.

Young, A. 1972. *Slopes*. Logman.